Advances in Cancer Biology - Metastasis 16 (2026) 100178

Contents lists available at ScienceDirect

Advances in Cancer Biology - Metastasis

journal homepage: www.journals.elsevier.com/advances-in-cancer-biology-metastasis

Integrative transcriptomic analysis of WNT/TGFβ-driven EMT pathways and drug-gene interaction networks in epithelial ovarian cancer

Roozbeh Heidarzadehpilehrood [a,*], King-Hwa Ling [b], Habibah Abdul Hamid [a]

[a] Department of Obstetrics & Gynecology, Faculty of Medicine and Health Sciences, Universiti Putra Malaysia, Serdang, 43400, Malaysia
[b] Department of Biomedical Science, Faculty of Medicine and Health Sciences, Universiti Putra Malaysia, Serdang, 43400, Malaysia

ARTICLE INFO

Keywords:
EMT biomarker
Epithelial ovarian cancer
Therapeutics
microRNA
Diagnostic
Systems biology

ABSTRACT

Background: Epithelial ovarian cancer (EOC) remains a lethal malignancy, and epithelial-mesenchymal transition (EMT) is a key driver of invasion, metastasis, and treatment resistance. Robust EMT-centered biomarkers in EOC are still lacking. We aimed to identify consensus EMT-related mRNA-miRNA signatures and drug-gene interactions across independent cohorts.

Methods: Three mRNA and one miRNA GEO datasets were analyzed. Differentially expressed genes (DEGs) were identified with limma and combined meta-analytically; consensus DEGs were directionally concordant with FDR <0.05. EMT involvement was evaluated using Hallmark EMT enrichment and correlations with EMTome-derived epithelial and mesenchymal scores in TCGA-OV. Functional enrichment, protein–protein interaction networks, hub genes, Human Protein Atlas validation, drug–gene interactions, and miRNA prediction and validation were integrated.

Results: We identified 528 consensus DEGs (131 up-regulated, 397 down-regulated) in EOC versus normal ovary. Up-regulated genes were enriched for EMT, extracellular matrix organization, and WNT/TGFβ/BMP signaling, whereas down-regulated genes involved signal transduction and cell-cell communication. Seventeen EMT-related genes, including NT5E, VIM, GAS1, and WNT5A, showed strong mesenchymal associations. Ten hub genes (AURKA, BIRC5, CDK1, EZH2, HMMR, IQGAP3, BCL2, DCN, NT5E, PGR) were consistently dysregulated, associated with poorer survival, and supported by protein-level differences. Integration with miRNA data highlighted ten EMT-related miRNAs, several with good diagnostic performance (AUC $\geq$0.80). Eight clinically relevant drug-gene pairs, including alisertib (AURKA) and venetoclax (BCL2), were prioritized.

Conclusions: This EMT-focused integrative analysis defines coherent mRNA-miRNA-drug axes in EOC. The identified EMT-regulatory modules provide candidate diagnostic and prognostic biomarkers and pathway-based therapeutic hypotheses that warrant validation in independent cohorts and functional models.

1. Introduction

Epithelial ovarian cancer is one of the deadliest gynecologic malignancies due to its frequent late-stage diagnosis and complex pathogenesis. It is the leading cause of death related to gynecologic malignancies in the United States and is ranked as the fifth most common cause of cancer mortality among women [1]. The disease is characterized by its heterogeneity, consisting of multiple histological subtypes, each harboring a distinct molecular and genetic profile [2]. These subtypes are further broadly classified into type I and type II tumors, in which type I is less aggressive and genetically stable, while type II tumors are highly aggressive, genetically unstable, and usually present with TP53 mutations [3]. Most of the EOC cases are diagnosed at an advanced stage, which contributes to the high mortality rate despite initial responsiveness to treatment [4]. The current management strategy involves a multidisciplinary approach: surgical cytoreduction and adjuvant chemotherapy. Emerging therapies focus on targeted treatments and maintenance therapies, including PARP inhibitors [1,5].

Proven studies have established that miRNAs may contribute to the development of EMT by modulating the process of gene expression that affects cancer progression and metastasis and even chemoresistance and could serve as potential biomarkers for early detection and diagnosis

This article is part of a special issue entitled: Drivers of EMT published in Advances in Cancer Biology - Metastasis.

* Corresponding author.
E-mail address: roozbeh.heidarzadeh@gmail.com (R. Heidarzadehpilehrood).

https://doi.org/10.1016/j.adcanc.2026.100178
Received 23 November 2025; Received in revised form 3 February 2026; Accepted 9 February 2026
Available online 10 February 2026

[6–9]. Staging in ovarian cancer establishes the prognostic value of lymph node dissection (LND), where, in the context of clinically early EOC, the survival advantage of LND is small while morbidity is significantly elevated, so a prognostic impact may be considered in a stage-specific fashion [10]. In addition to a purely anatomic factor, the tumor microenvironment, especially the immune microenvironment in metastases, plays a significant role in progression as well as response to treatment, as immune cell characterization has been correlated with outcome [11]. Additionally, endocrine-immune interactions through receptor-mediated mechanisms can modify both the microenvironments and the process of metastasis [12]. Knowledge of molecular pathogenesis and extraovarian origins of EOC thus becomes absolutely necessary for devising effective prevention and treatment strategies [3].

MicroRNAs and messenger RNAs are important regulators in the

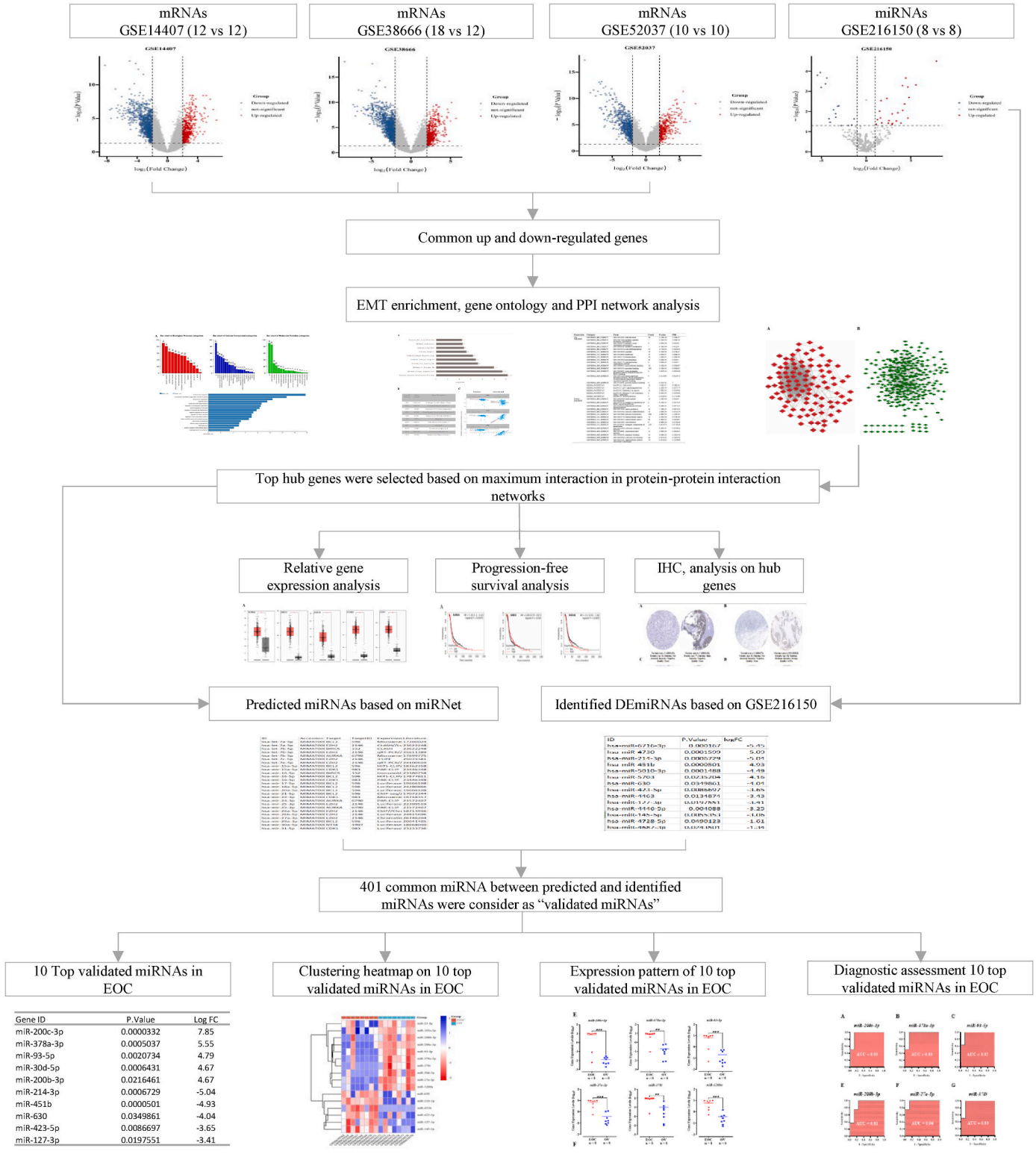

Gene ID	P.Value	Log FC
miR-200c-3p	0.0000332	7.85
miR-378a-3p	0.0005037	5.55
miR-93-5p	0.0020734	4.79
miR-30d-5p	0.0006431	4.67
miR-200b-3p	0.0216461	4.67
miR-214-3p	0.0006729	-5.04
miR-451b	0.0000501	-4.93
miR-630	0.0349861	-4.04
miR-423-5p	0.0086697	-3.65
miR-127-3p	0.0197551	-3.41

Fig. 1. Illustrates a workflow of three mRNAs cohorts (GSE1440, GSE38666, GSE52037; Affymetrix GPL570) and (GSE216150, Agilent miRNA) transcriptomic analyses were conducted with in study and meta combined across cohorts in epithelial ovarian cancer.

pathogenesis and development of epithelial ovarian cancer, one of the most lethal gynecological malignancies. MicroRNAs are small non-coding RNA molecules that regulate the expression of their target genes through specific binding to mRNAs, leading to mRNA degradation or suppression of translation [13–15]. Aberrant expression of miRNAs is associated with all aspects of tumor biology, including metastasis, chemoresistance, and disease progression in EOC [14–16]. For example, the miR-200 family may modulate metastasis and chemoresistance in EOC and therefore have therapeutic potential [17]. Further, miR-205, miR-200c, and miR-141 are potential biomarkers of early diagnosis of EOC due to their stability in circulation and being significantly differentially expressed in malignant tissues compared to normal tissues [18, 19]. The complexity of miRNAs-mRNAs relationship is interfered with by lncRNAs, which may set up some sort of regulatory network contributing to drug resistance and tumor progression [20,21]. These complex interactions among miRNAs, mRNAs, and lncRNAs in EOC take roots from a critical foundation that needs to be determined if new diagnostic and therapeutic strategies against EOC are to be achieved. Our innovation consists of a regulatory, therapy-focused framework of EMT in EOC, emphasizing actionable WNT and TGFβ/BMP modules and converting them into refined drug-gene hypotheses.

2. Materials and methods

2.1. Data mining and normalization

Fig. 1 illustrates a workflow of transcriptomic analysis on the clinical samples of epithelial ovarian cancer compared to normal ovarian samples. The raw data were obtained from the GEO database by utilizing the R package GEOquery and the getGEO function, which enabled downloading raw gene expression profiles from datasets GSE14407, GSE38666, GSE52037, and GSE216150. In this study, the EOC samples were obtained from epithelial ovarian carcinoma, while the OV samples obtained from healthy controls. We evaluated three mRNA cohorts: GSE14407 (12 EOC/12 normal), GSE38666 (18/12), and GSE52037 (10/10), all utilizing Affymetrix GPL570 (HG-U133 Plus 2.0 microarray platforms). We selected the microRNA microarray GSE216150 (8/8) with Agilent GPL20712. We employed RMA processing for Affymetrix chips (background correction, quantile normalization, and log2 transformation); utilized HGNC symbols (maximum IQR for multi-probe genes); and applied the limma empirical Bayes test for differential expression analysis for each dataset. Gene effects were meta-analytically aggregated across datasets using random effects on log fold changes or Fisher's test on *p-values* as appropriate.

2.2. Differential expressed genes (DEGs)

MetaMA was used to detect the intersection among the DEGs from three datasets, namely, GSE14407, GSE38666, and GSE52037, through meta-analysis. Overlapping DEGs were drawn using the R package VennDiagram, where the function draw.triple.venn() depicted common DEmRNAs in those datasets. GSE216150 dataset: Raw data from the Agilent-070156 human miRNA microarray platform was analyzed using the limma package. Data normalization was done by using the function normalizeBetweenArrays() to make technical variations between the same sample comparable. The DEmiRNAs had been identified based on $|\log2\ FC| > 2$ and adjusted $p\text{-}value < 0.05$.

2.3. EMT pathway definitions and enrichment

Our two-fold strategy connected transcriptome data to biological processes of epithelial to mesenchymal transition (EMT). First, we examined consensus tumor up/down-regulated genes in all three mRNA sets (GSE14407, GSE38666, GSE52037). To reduce inter-dataset variability across heterogeneous microarray cohorts, a stringent differential expression threshold was applied, thereby prioritizing robust and consistently dysregulated genes for downstream EMT-focused analyses. The Hallmark gene set library was used to analyze the set of 76 dysregulated consensus tumor DEGs on the Gene Set Enrichment Analysis (GSEA)/Molecular Signature Database (MSigDB) web platform, which returned results as -log10 the false discovery rate (FDR) using default parameters. Second, we used pre-computed scores from the EMTome online site, which provides TCGA-based EMT signatures and NES values for numerous cancers, including ovarian cancer (TCGA-OV), to evaluate EMT-related pathways at the patient level. NES values of the "Epithelial top 50 genes" and "Mesenchymal top 50 genes" signatures, as well as log2 transformed values of RNA expression (log2(expression + 1)), were extracted for the top 17 EMT-related consensus genes that emerged after intersecting our set of up-regulated DEGs (76 genes) with the Hallmark EMT gene set in the MSigDB. Gene expression and epithelial and mesenchymal NES values were correlated using Spearman's rank correlation coefficients for the top 17 EMT-related consensus genes. The Benjamini & Hochberg FDR procedure was used to identify genes with an FDR <0.05 in at least one EMT-related program, indicating significant association with EMT activity.

2.4. Gene ontology enrichment analysis

All the common DEGs from GSE14407, GSE38666, and GSE52037 were identified for gene ontology analysis. GO, including biological process (BP), cellular component (CC) and molecular function (MF) (https://maayanlab.cloud/enrichr-kg), with an FDR <0.05 considered statistically significant [22].

2.5. Protein-protein network and module analysis

The common differentially expressed genes (DEGs) identified from the GSE14407, GSE38666, and GSE52037 datasets were selected for protein-protein interaction (PPI) analysis. We included only DEGs that had an adjusted $p\text{-}value < 0.05$ and $|\log2\ FC| \geq 2$ which were consistently dysregulated across all three datasets. The PPI networks were constructed using the STRING database (version 12.0, https://string-db.org) with a medium confidence score threshold of 0.4 and no additional interactors (maximum number of interactors = 0). The resulting PPI networks were visualized and analyzed in Cytoscape (version 3.9.1, https://cytoscape.org/). Furthermore, 12 CytoHubba topological algorithms were employed to identify the most significant hub genes and subnetworks within the PPI network [23].

2.6. Transcriptomic signature and survival analysis

We applied specific inclusion and exclusion criteria to the patient data, which included accessible overall survival (OS) and progression-free survival (PFS) statistics, as well as corresponding gene expression profiles for the study. The KM-Plotter tool automatically excluded samples that lacked survival time, survival status, or RNA expression data. Additionally, only patients diagnosed with epithelial ovarian cancer were included. We utilized the GEPIA tool (http://gepia.cancer-pku.cn/) for analysis. The criterion of log-rank $p\text{-}value < 0.05$ was employed to evaluate hub genes related to progression-free survival using the widely recognized Kaplan-Meier plotter tool, which incorporates data from TCGA, EGA, and GEO databases (https://kmplot.com/analysis/) [24].

2.7. Immunohistochemistry (IHC) analysis

The top 10 hub proteins identified from the CytoHubba network analysis were selected for protein expression profiling using the Human Protein Atlas (HPA, version 23.0, https://www.proteinatlas.org/). HPA tumor and normal tissues were collected from both patients and healthy individuals; consequently, IHC serves as an orthogonal method for protein-level validation rather than as paired references. Only proteins

with available IHC data for normal ovarian and ovarian cancer tissues were included in the analysis. Protein expression levels were classified into four categories high, medium, low, and not detected based on the standardized HPA scoring system. This grading system combines the percentage of stained cells (>75%, 25-75%, or <25%) and staining intensity (strong, moderate, weak, or negative), as described previously [25].

2.8. Gene-drug interaction analysis

The top 10 hub genes were further analyzed for potential drug–gene interactions using the Drug-Gene Interaction Database (DGIdb, version 5.0, https://dgidb.org/). Only interactions supported by curated databases and FDA-approved drugs were considered. Candidate compounds were filtered based on therapeutic relevance, including hormonal agents, antineoplastic agents, selective estrogen receptor modulators (SERMs), and immunosuppressants. We ensured that drug mechanisms of action were concordant with the direction of target dysregulation by harmonizing gene symbols to HGNC and drugs to WHO INN, getting rid of duplicates, and making sure that drug MoA and target biology were in sync (etoposide/teniposide/epirubicin TOP2A; tamoxifen/toremifene ESR1; goserelin GNRHR). Entries that weren't supported or were contradictory were left out. Table 1 shows the actionable subset.

2.9. miRNA prediction and assessment

The top 10 genes were assessed for the prediction of miRNAs using the miRNet tool (version 2.0, https://www.mirnet.ca/miRNet/home.xhtml). Only miRNAs with a degree cutoff of 1.0 and a betweenness centrality threshold of 1.0 were considered. We retained only miRNAs with experimental support in miRTarBase/miRNet and inverse expression trends relative to their predicted targets. The differentially expressed miRNAs (DE-miRNAs) identified in the GSE216150 repository were used as a resource for the external validation of predicted miRNAs in epithelial ovarian tissue as compared to OV tissue.

2.10. Statistical analyses

R software (version 4.2.2) was used for all data processing and analysis. A stringent |log2FC| threshold (>2) was applied to prioritize genes with large and biologically meaningful expression changes. Statistically, this cutoff was chosen to reduce noise and false-positive results arising from inter-platform and inter-cohort heterogeneity inherent to meta-analyses of microarray datasets. The Wilcoxon rank-sum test was used to compare two groups. The Spearman correlation analysis was used to ascertain the correlation coefficients among different substances. Unless noted, significance used BH-FDR ($q < 0.05$). Volcano plots show -log10 (adjusted p-value) vs log2 FC. Enrichment tested by Fisher with BH-FDR across modules.

3. Results

3.1. Dataset summary

Supplementary File 1 shows a summary of the datasets (GEO IDs, platforms, case/control counts). Analyses were done both within the study and in a meta-combined way.

3.2. Differentially expressed genes in EOC

In Fig. 2, panels A-C display the transcriptomic profiles for the datasets. A total of 3385 DEmRNAs were obtained from GSE14407, GSE38666, and GSE52037. Genes were considered significantly dysregulated if adjusted p-value <0.05 and |log2FC| > 2 (528 including 131 up/397 down-regulated). Rather than pooling raw arrays across platforms, we performed within-study differential expression and then combined gene-level effects meta-analytically, which reduces cross-platform batch artefacts. Lower fold-change thresholds were not systematically pursued, as the analysis was designed to prioritize robust and reproducible transcriptional alterations across heterogeneous datasets. Fig. 2D volcano plot of transcriptomic profiles of miRNAs in GSE216150, including a total of 2092 DEmiRNAs. 397 common DEGs were consistently down-regulated across all three datasets, while 131 common DEGs were up-regulated (Fig. 2E and F).

3.3. EMT characteristics and sample-level EMT engagement

We then investigated if the consensus tumor dysregulated genes reflected EMT-related biology in epithelial ovarian cancer. The 76 EMT-consensus genes were obtained by intersecting the differentially expressed genes with the Hallmark EMT gene set from MSigDB. (Fig. 3A). The EMT pathway had the strongest signal (−log10 FDR ~ 13–14) when enrichment was summarized as -log10 (FDR). This means that the FDR was well below 10^{-13}. Other programs that were enriched were Estrogen Response Late (-log10 FDR ~ 10), UV Response Down (~9), KRAS Signaling Up (~8), Androgen Response (~7), Estrogen Response Early (~6-7), Apoptosis (~6), Coagulation (~5), Adipogenesis (~3), and Bile Acid Metabolism (~2).

Among the 17 EMT-related consensus genes, a subset showed particularly strong associations with EMT scores (Fig. 3B). EZH2 exhibited only weak correlations with EMT scores, showing a modest negative association with epithelial NES ($R = -0.12$, *p-value* $= 0.03$) and no significant correlation with mesenchymal NES ($R = -0.061$, *p-value* $= 0.29$). This indicates that, within this dataset, EZH2 expression is not closely linked to either epithelial or mesenchymal TCGA signatures. GAS1 exhibited a robust positive correlation with mesenchymal NES ($R = 0.55$, *p-value* $< 2.2 \times 10^{-16}$), whereas its correlation with epithelial NES was weak and statistically insignificant ($R = -0.11$, *p-value* $= 0.06$, Fig. 3C).

Table 1
Candidate drugs based on the gene (HGNC), drug (INN) interaction.

Drug (INN)	Gene (HGNC)	Target class/Mechanism	Direction-of-effect	Regulatory approval	Indication (principal)
Alisertib (MLN8237)	AURKA	Aurora A kinase inhibitor	inhibitor	Investigational	Solid tumors/hematologic (investigational)
Teniposide	TOP2A	Topoisomerase II poison/intercalator	inhibitor	Approved	Antineoplastic (various)
Etoposide	TOP2A	Topoisomerase II poison/intercalator	inhibitor	Approved	Antineoplastic (various)
Epirubicin	TOP2A	Topoisomerase II poison/intercalator	inhibitor	Approved	Antineoplastic (various)
Tamoxifen	ESR1	Selective estrogen receptor modulator (SERM)	antagonist/partial agonist	Approved	Hormone receptor positive breast cancer
Toremifene	ESR1	Selective estrogen receptor modulator (SERM)	antagonist/partial agonist	Approved	Hormone receptor positive breast cancer
Goserelin	GNRHR	GnRH agonist (pituitary down-regulation)	agonist	Approved	Hormonal therapy (breast/prostate)
Venetoclax	BCL2	BCL2 inhibitor	inhibitor	Approved	CLL/SLL; AML

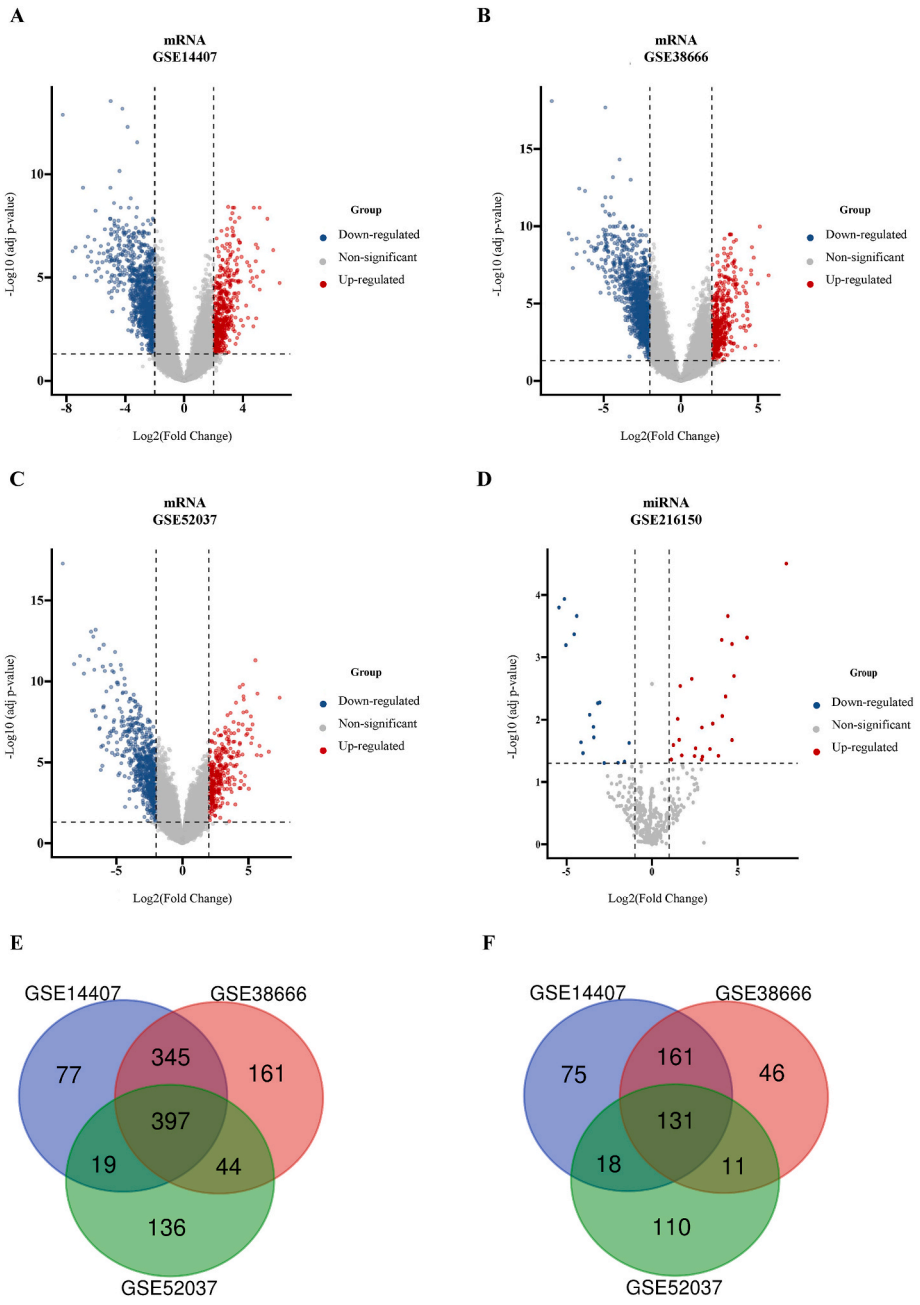

Fig. 2. Illustrates the differential expression of genes (DEGs) and common hub genes in epithelial ovarian cancer (EOC) compared to normal ovarian tissues (OV). **A-D** The volcano plots illustrated the differentially expressed mRNAs and miRNAs in each dataset in EOC vs. OV. **E** & **F** A total of 131 common up-regulated and 397 common down-regulated DEGs were identified in the three datasets (GSE14407, GSE38666, and GSE52037) between EOC vs. OV with the following criteria: |log2 FC| > 2, adjusted *p-value* < 0.05.

3.4. Gene ontology analysis in EOC

We next explored the biological programs shared across datasets by performing functional enrichment on the consensus DEGs that were directionally concordant in all three cohorts. The common up-regulated genes (Fig. 4A) were significantly enriched for pathways related to extracellular matrix (ECM) organization, tissue remodeling and developmental signaling, including terms such as regulation of ossification, extracellular matrix organization and Wnt/TGF-β/BMP-related signaling (ranked by -log10 FDR). These enrichments are consistent with an invasive, pro-EMT tumor phenotype, highlighting activation of matrix-remodeling and morphogenesis programs in epithelial ovarian cancer. In contrast, the common down-regulated genes (Fig. 4B) showed over-representation of broader signal transduction and cell-cell communication pathways, including generic signal transduction, G-protein coupled receptor/neuropeptide signaling and related communication modules, again ordered by -log10 FDR.

3.5. Protein-protein interaction networks in EOC

A total of 405 nodes with a confidence value exceeding 0.4 were incorporated into the PPI networks, comprising 104 nodes and 818 edges for up-regulated proteins, and 301 nodes and 668 edges for down-regulated genes (Fig. 5A and B, and Supplementary Files 4 & 5). Subsequently, a refined PPI network using the cytoHubba plugin was illustrated, which consisted of 50 nodes and 718 edges for up-regulated genes, and 118 nodes and 301 edges for down-regulated DEGs (Fig. 5C and D). Furthermore, the top 10 up- and down-regulated hub genes were

A

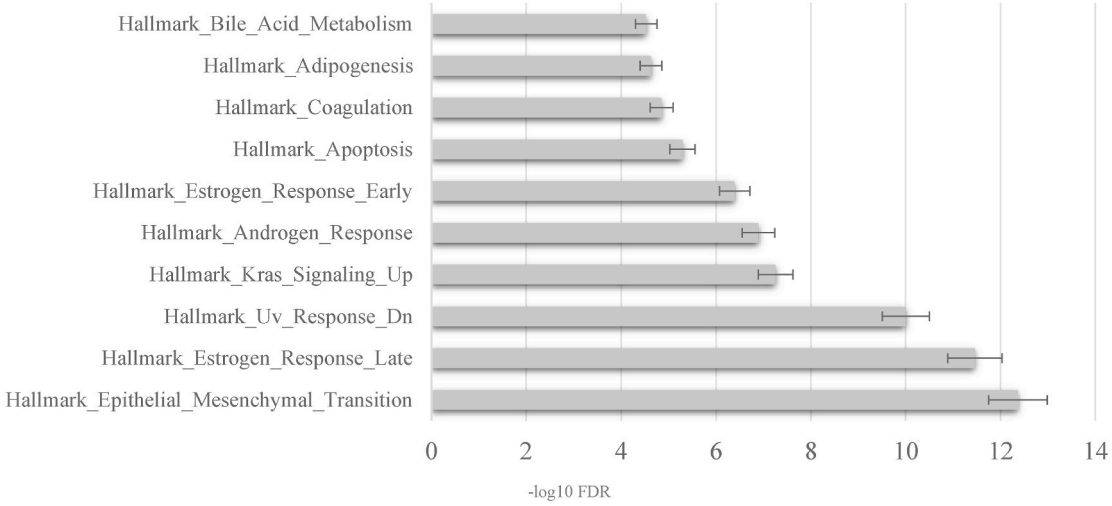

B

Gene ID (Entrez)	Gene Symbol	Gene Description
1281	COL3A1	Collagen Type III Alpha 1 Chain
5376	PMP22	Peripheral Myelin Protein 22
5999	RGS4	Regulator Of G Protein Signaling 4
6591	SNAI2	Snail Family Transcriptional Repressor 2
7980	TFPI2	Tissue Factor Pathway Inhibitor 2
1634	DCN	Decorin
5396	PRRX1	Paired Related Homeobox 1
667	DST	Dystonin
2619	GAS1	Growth Arrest Specific 1
7474	WNT5A	Wnt Family Member 5A
1842	ECM2	Extracellular Matrix Protein 2
25890	ABI3BP	ABI Family Member 3 Binding Protein
4256	MGP	Matrix Gla Protein
5744	PTHLH	Parathyroid Hormone Like Hormone
6422	SFRP1	Secreted Frizzled Related Protein 1
6695	SPOCK1	SPARC (Osteonectin), Cwcv And Kazal Like Domains Proteoglycan 1
7431	VIM	Vimentin

C

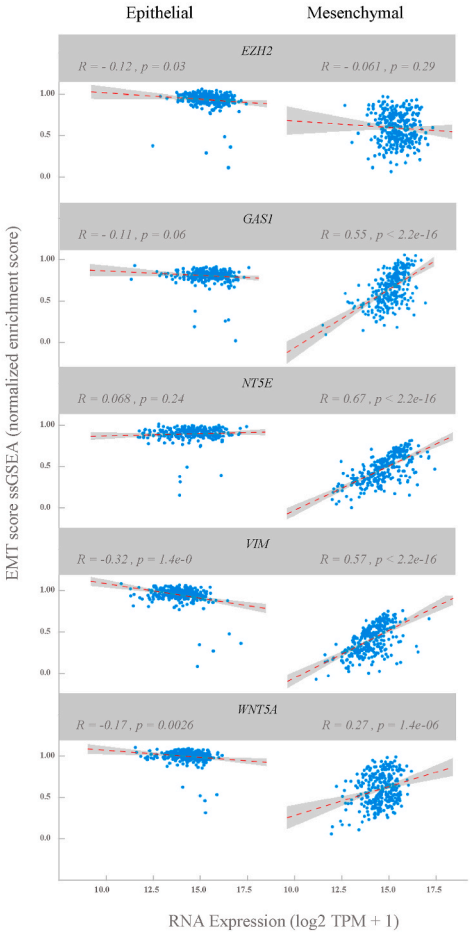

Fig. 3. Enrichment of consensus genes in EMT, association of EMT signatures to epithelial and mesenchymal epithelial ovarian cancer. **A** Enrichment of tumor dysregulated genes to Hallmark pathways (-log10 FDR) for identifying consensus tumor dysregulated genes in the three EOC datasets (76 genes). **B** The enrichment of consensus tumor dysregulated genes to the MSigDB Hallmark gene set for EMT (17 gene enrichment). The common set of genes (*COL3A1, PMP22, RGS4, SNAI2, TFPI2, DCN, PRRX1, DST, GAS1, WNT5A, ECM2, ABI3BP, MGP, PTHLH, SFRP1, SPOCK1,* and *VIM*) is recognized as EMT-related consensus genes, which now proceed to integration with GSEA database scores for functional annotation analysis. **C** Correlation between EMT signature scores and transcriptomic expressions of EMT-related consensus genes in TCGA ovarian samples by using GSEA (Spearman's R). The x-axis is for log2 transformation of TPM for visualization of data in logarithm scale (Log2 TPM + 1). Only those genes that showed significant association to either EMT signatures of the web platform EMTome or MSigDB are listed in this figure.

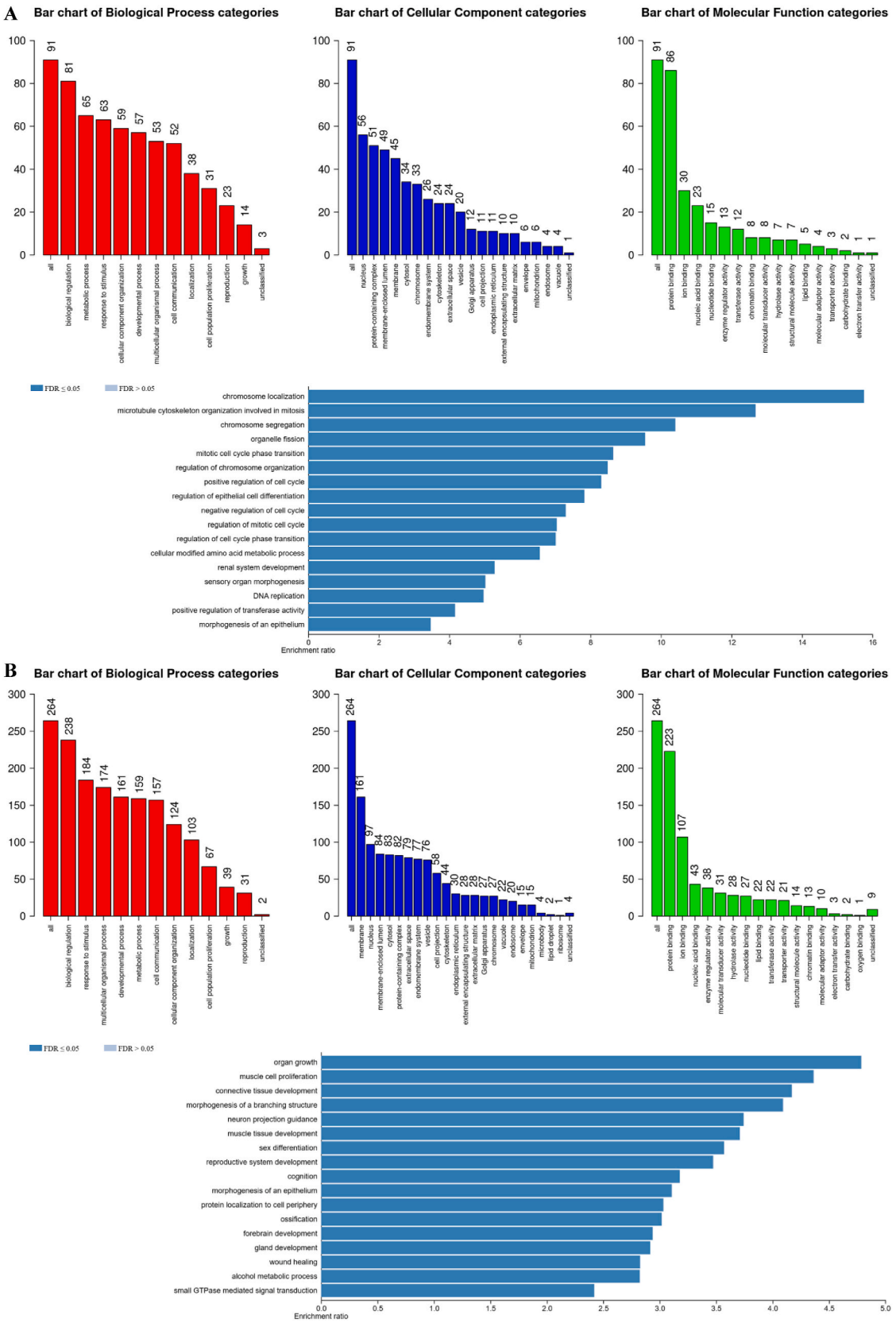

Fig. 4. Shared biological pathways associated with consensus differentially expressed genes across three epithelial ovarian cancer cohorts. Consensus genes were defined as significantly differentially expressed (FDR <0.05) and directionally concordant in all three datasets. **A** Bar plot of the top enriched Gene Ontology Biological Process 2021 and Reactome 2022 pathways for the common up-regulated genes. Prominent categories include extracellular matrix organization, regulation of ossification, and Wnt/TGF-β/BMP-related developmental signaling, consistent with activation of matrix-remodeling and EMT-like programs in tumor tissue. **B** Over-represented terms include broad signal transduction modules, cell-cell communication, and neuropeptide/GPCR signaling. Bars represent -log10 (FDR-adjusted *p-value*), and only pathways with FDR <0.05 are shown.

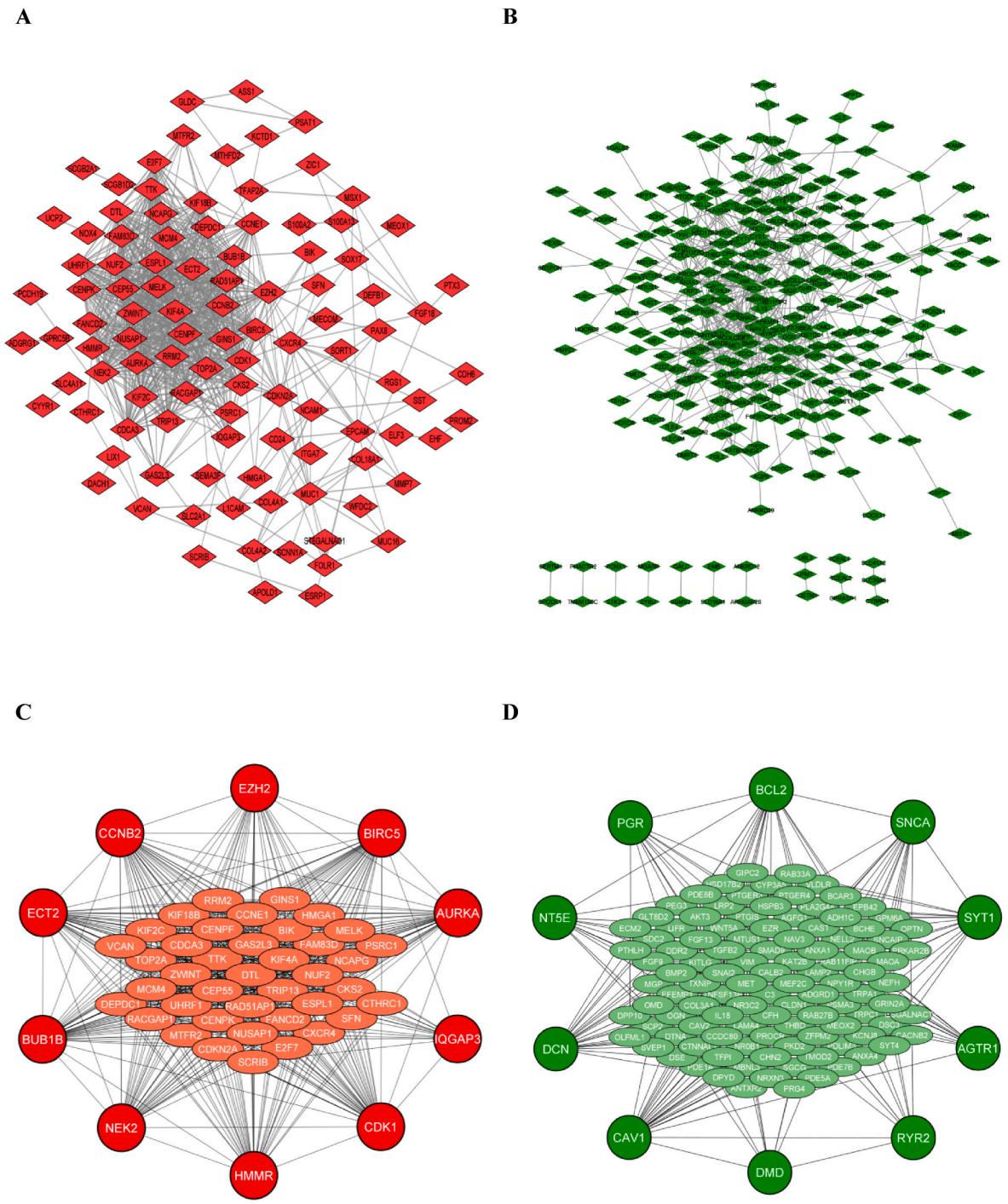

Fig. 5. Protein-protein interaction (PPI) network construction of hub genes. **A** PPI network of up-regulated DEGs contained 104 nodes and 818 edges. **B** A protein-protein network of down-regulated DEGs contained 301 nodes and 668 edges. **C** & **D** Significantly up- and down-regulated hub genes (circle nodes) and subnetworks (oval nodes) were retrieved from cytoHubba analysis. The red nodes represented up-regulated genes. The green nodes represented down-regulated genes.

obtained utilizing 12 CytoHubba topological modules.

3.6. Transcriptomic signature and survival analysis in EOC

A total of 6 hub mRNAs, including *AURKA, BIRC5, CDK1, EZH2, HMMR,* and *IQGAP3*, consistently showed an up-regulated pattern in EOC compared to the OV, while the remaining 4 top mRNAs, including *BCL2, DCN, NT5E,* and *PGR*, consistently showed a down-regulated pattern in EOC tissues vs. normal OV (*p-value* < 0.05, Fig. 6A). The survival values of the six up-regulated hub genes *AURKA, BIRC5, CDK1, EZH2, HMMR*, and *IQGAP3* and four down-regulated hub genes revealed significant progression-free survival rates (*p-value* < 0.05, Fig. 6B).

3.7. IHC analysis in EOC

The antibodies were utilized to evaluate the expression levels of six up-regulated hub proteins (AURKA, BIRC5, CDK1, EZH2, HMMR, and IQGAP3) and four down-regulated hub proteins (BCL2, DCN, NT5E, and PGR) in ovarian cancer tissues compared to normal ovarian tissues. The protein expression values of *AURKA, BIRC5, CDK1, EZH2, HMMR*, and

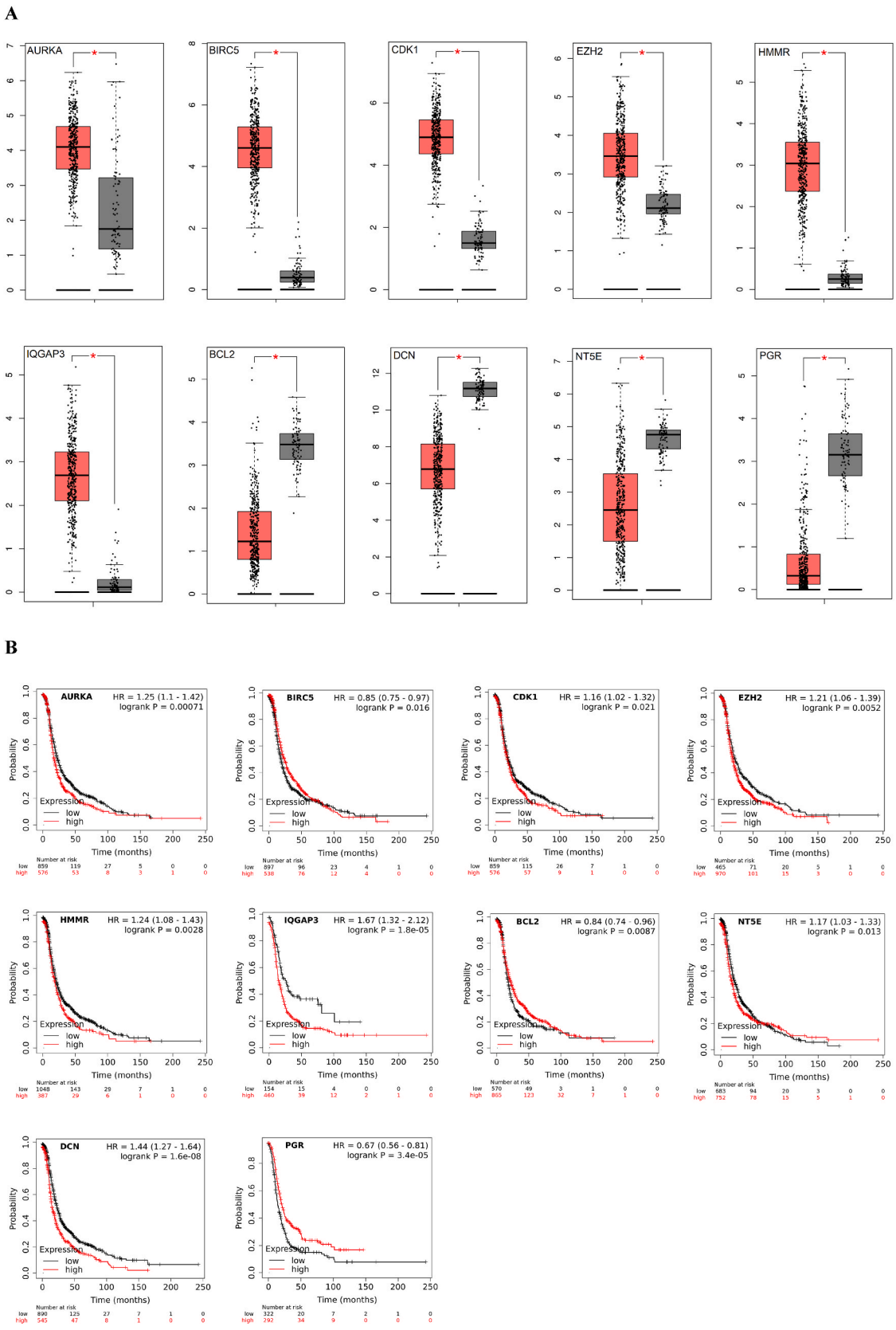

Fig. 6. Gene expression profile and survival analysis of top 10 up- and down-regulated hub genes between EOC and normal OV. **A** The top 10 hub genes exhibited a strong overexpression pattern in EOC vs. normal OV tissues. All hub genes were assessed using the GEPIA dataset. The red color represents tumor tissues (n = 426), while the gray color denotes normal tissues (n = 88) (*p-value* < 0.05). **B** Prognostic survival analysis of 10 hub genes in EOC vs. normal OV was assessed using Kaplan-Meier plotter. The ten most significantly up- and down-regulated hub genes' survival values in EOC vs. normal OV tissues.

IQGAP3 were found to be higher in ovarian cancer tissues compared to normal ovarian tissues (Fig. 7A–F), whereas the protein expression values of *BCL2, DCN, NT5E,* and *PGR* were found to be lower in ovarian cancer tissues compared to normal ovarian tissues, respectively (Fig. 7G–J).

3.8. Candidate drugs based on the gene-drug interaction in EOC

A total of 10 genes were used to identify drug repurposing hypotheses; we retained eight unique drug-gene pairs with mechanistically consistent interactions (Table 1). Most interactions involve approved agents (7/8; 87.5%), indicating mechanistically plausible drug-gene links, alongside one investigational AURKA inhibitor (Alisertib). There are four functional classes of targets: DNA topology (TOP2A) with three approved cytotoxics (etoposide, teniposide, and epirubicin); a cell-cycle kinase (AURKA) that is inhibited by alisertib; nuclear hormone receptors (ESR1) that are modulated by SERMs (tamoxifen and toremifene); the endocrine GPCR axis (GNRHR) that is engaged by goserelin; and the apoptosis regulator BCL2 that is inhibited by venetoclax. The direction of effect is in line with the biology of the target (inhibitors 5/8, antagonist/partial agonist 2/8, agonist 1/8), which is in line with a context that promotes cell growth and regulates EMT.

3.9. miRNAs prediction and assessment in EOC

A total of 1006 miRNAs were predicted based on the 10 hub genes (Supplementary File 6). A total of 2092 DEmiRNAs were obtained from GSE216150 with a cutoff of *p-value* < 0.05 (Supplementary File 7). The Venn tool was used to identify 401 common miRNAs between predicted miRNAs and pre-existing miRNAs (Fig. 8A and Supplementary File 8). The top 10 significant miRNAs were selected (Fig. 8B). A clustering heatmap was constructed to visualize top DEmiRNAs in EOC (Fig. 8C). A total of 10 top and common miRNAs were selected, and transcriptomic expression profiles of those were assessed on epithelial ovarian cancer, including miR-200c-3p, *p-value* < 0.001, 95% CI: 3.479-10.90 vs. 0.004-0.021; miR-378a-3p, *p-value* $= 0.002$, 95% CI: 4.446-10.36 vs. 4.27e-005-0.404; miR-93-5p, *p-value* < 0.001, 95% CI: 3.319-10.20 vs. 0.014-0.390; miR-30d-5p, *p-value* $= 0.007$, 95% CI: 5.621-10.96 vs. −1.315-4.200; miR-200b-3p, *p-value* $= 0.038$, 95% CI: 5.621-10.96 vs. −1.315-4.200; miR-214-3p, *p-value* $= 0.004$, 95% CI: 0.029-1.100 vs. 1.852 vs. 9.779; miR-451b, *p-value* < 0.001, 95% CI: −1.237-6.368 vs. 8.932-9.744; miR-630, *p-value* $= 0.038$, 95% CI: −1.473-3.758 vs. −0.245-7.162; miR-423-5p, *p-value* $= 0.004$, 95% CI: 0.061-0.430 vs. 1.793-8.929; and miR-127-3p, *p-value* $= 0.005$, 95% CI: −1.037-3.784 vs. 3.33-9.868 (Fig. 8D).

3.10. ROC analysis of miRNAs in EOC

To evaluate the possible diagnostic relevance of the identified miRNA expression status for distinguishing between epithelial ovarian cancer and ovarian tissue, ROC analyses were carried out. The analyses reported miR-200c-3p, AUC = 0.93, 95% CI: 0.80 to 1.00; miR-378a-3p, AUC = 0.93, 95% CI: 0.80 to 1.00; miR-93-5p, AUC = 0.92, 95% CI: 0.78 to 1.00; miR-30d-5p, AUC = 0.89, 95% CI: 0.72 to 1.00; miR-200b-3p, AUC = 0.81, 95% CI: 0.57 to 1.00; miR-214-3p, AUC = 0.92, 95% CI: 0.79 to 1.00; miR-451b, AUC = 0.76, 95% CI: 0.48 to 1.00; miR-630, AUC = 0.81, 95% CI: 0.57 to 1.00; miR-423-5p, AUC = 0.87 and miR-127-3p, AUC = 0.90 (Fig. 8E).

4. Discussions

In this study, we integrated three independent mRNA datasets and one miRNA dataset to define a consensus EMT-centered transcriptomic signature in epithelial ovarian cancer. Across cohorts, we identified 528 differentially expressed genes (131 up-regulated and 397 down-regulated in EOC vs. normal ovarian tissue), alongside a compact panel of ten hub genes and ten candidate miRNAs. By combining Hallmark EMT enrichment, EMTome-derived epithelial and mesenchymal scores, PPI network topology, survival analysis, and drug-gene interactions, we moved from a long list of DEGs towards a regulatory and therapy-oriented framework for EMT in EOC. Our enrichment analyses indicate that the consensus up-regulated genes converge on extracellular matrix (ECM) organization, EMT, and developmental signaling programs, particularly WNT and TGFβ/BMP pathways.

Epithelial ovarian cancer encompasses multiple histological subtypes, including high-grade serous, endometrioid, clear cell, and mucinous carcinomas, each characterized by distinct molecular features. Due to incomplete and inconsistent subtype annotation across the public transcriptomic datasets analyzed in this study, EOC was evaluated as a single entity. This heterogeneity may influence EMT-associated signals, hub gene prioritization, and survival associations, and therefore represents a limitation of the present analysis. In addition, EMT is increasingly recognized as a dynamic and plastic process that often occurs as partial or hybrid epithelial-mesenchymal states rather than a complete phenotypic transition. In this study, EMT is therefore consider from integrated transcriptomic patterns and pathway-level signatures, rather than being directly demonstrated through functional or morphological assays. Accordingly, our findings should be interpreted as evidence of EMT-associated transcriptional activity and regulatory engagement, rather than direct experimental validation of EMT itself.

These findings are consistent with the notion that EOC aggressiveness is driven not only by proliferative signaling but also by matrix remodeling, tissue plasticity, and changes in cell-cell and cell-matrix adhesion [26]. In contrast, the down-regulated consensus genes were enriched in broader signal transduction and neuropeptide/GPCR-related communication pathways, suggesting a loss of homeostatic signaling that may normally constrain tumor progression. Taken together, these patterns support a model in which EOC tumors adopt an EMT-like, pro-invasive state characterized by active ECM and morphogen signaling and concomitant attenuation of regulatory communication networks. By intersecting our consensus DEGs with the Hallmark EMT set and correlating them with EMTome signatures, we identified a subset of EMT-related consensus genes with strong functional links to EMT biology. NT5E (CD73), VIM, GAS1, and WNT5A showed robust positive correlations with mesenchymal pathways, whereas their association with epithelial signatures was weak or absent.

This is consistent with the previously defined functions of vimentin and the non-canonical WNT signaling pathway within the promotion of mesenchymal phenotypes and invasive potential for EOC [27,28]. GAS1, which presented a very strong correlation with mesenchymal NES and not with epithelial NES, may be a less well-studied EMT effector transcript within ovarian cancer [29]. Others, such as EZH2, presented modest and not significant correlations with the EMT scores, and thus indicate that, even if deregulated within EOC and of key importance, the contribution of such factors may be addressed through the action of chromatin and epigenetic remodeling [30,31].

Based on the PPI networks and CytoHubba, we identified the list of ten hub genes that are common to both networks and show poor prognosis: AURKA, BIRC5, CDK1, EZH2, HMMR, IQGAP3, BCL2, DCN, NT5E, and PGR. The expression level of six hub genes (AURKA, BIRC5, CDK1, EZH2, HMMR, and IQGAP3) was shown to be up-regulated in EOC, while the other four (BCL2, DCN, NT5E, and PGR) were found to be down-regulated. Several of these genes have already been shown to be involved in cell cycle regulation, apoptosis, and EMT events within ovarian and other cancers. AURKA is a Ser/Thr kinase that participates in the entry into mitosis, the maturation of centrosomes, and the segregation of chromosomes [32]. Its overexpression has been linked to genomic instability, aggressiveness of the clinicopathological characteristics, and a poor prognosis for various cancers, such as ovarian cancer [33,34]. As shown in the analysis presented, the overexpression of the gene AURKA correlated with a poor progression-free survival and the elevated expression of the protein AURKA within the tumor vs.

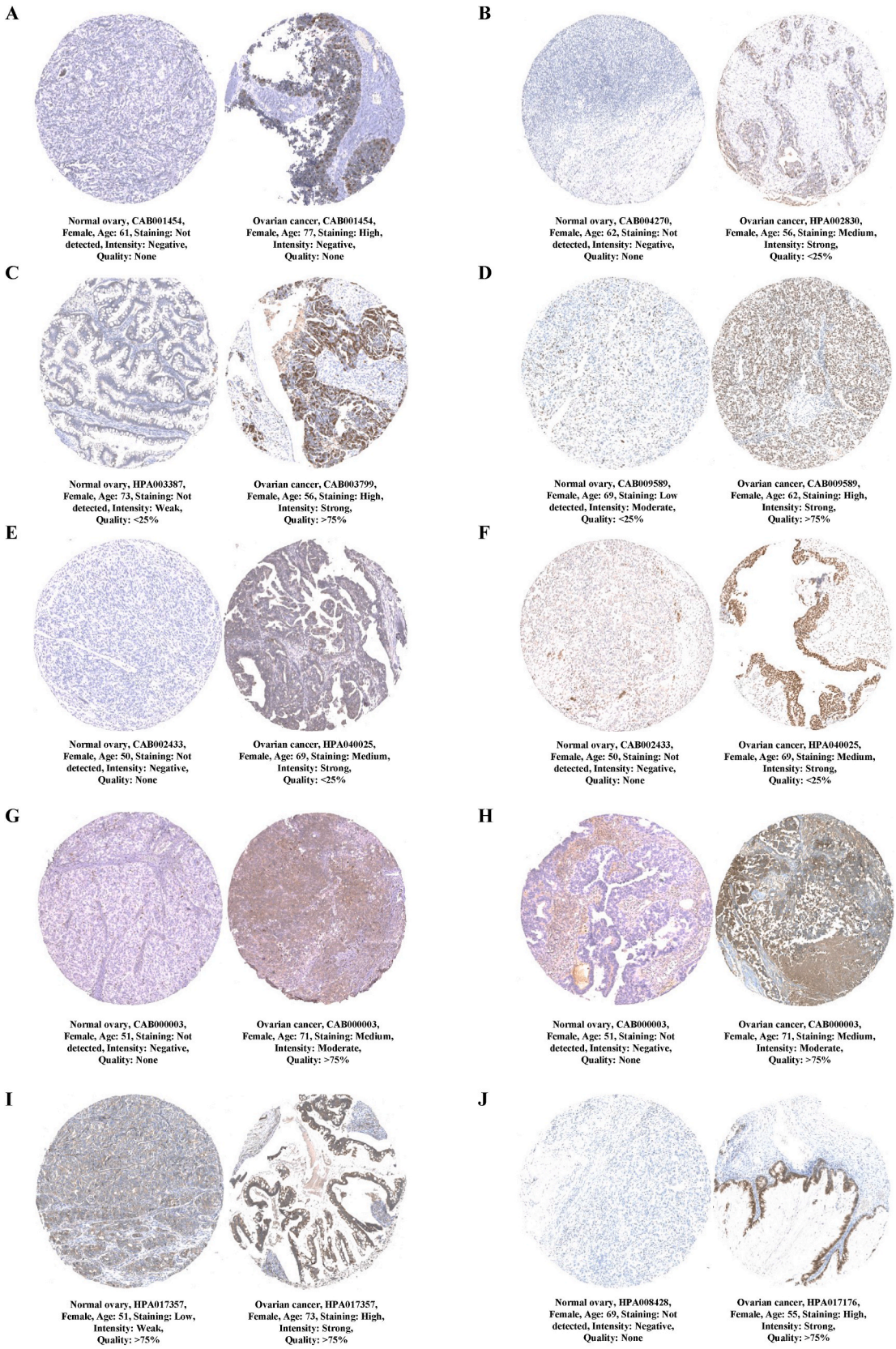

Fig. 7. Immunohistochemistry (IHC) analysis illustrating the tissue-specific protein expression levels of hub genes based on the Human Protein Atlas (HPA) website. **A-J** Protein expression levels of *AURKA*, *BIRC5*, *CDK1*, *EZH2*, *HMMR*, *IQGAP3*, *BCL2*, *DCN*, *NT5E*, and *PGR* in normal ovarian tissue compared to ovarian cancer tissue, respectively, HPA normal and tumor panels drive from different donors used for orthologue corroboration.

A

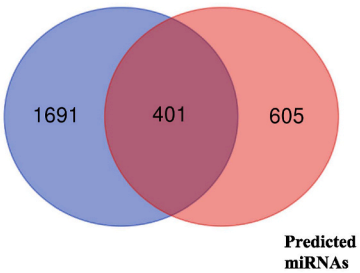

B

Gene ID	*P.Value*	Log FC
miR-200c-3p	0.0000332	7.85
miR-378a-3p	0.0005037	5.55
miR-93-5p	0.0020734	4.79
miR-30d-5p	0.0006431	4.67
miR-200b-3p	0.0216461	4.67
miR-214-3p	0.0006729	-5.04
miR-451b	0.0000501	-4.93
miR-630	0.0349861	-4.04
miR-423-5p	0.0086697	-3.65
miR-127-3p	0.0197551	-3.41

C

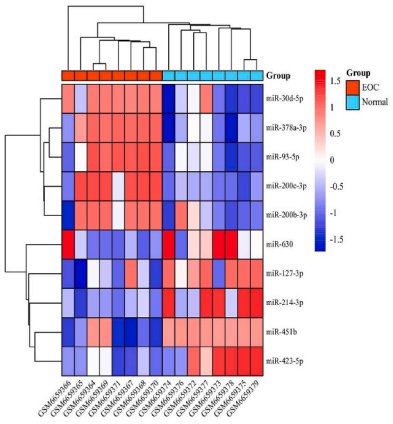

D

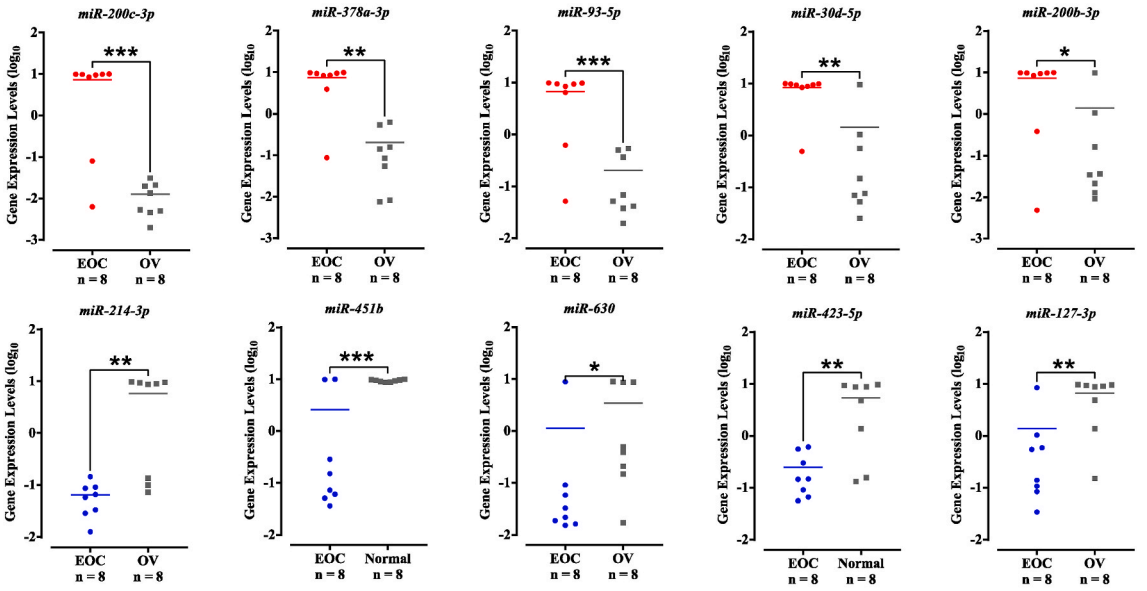

E

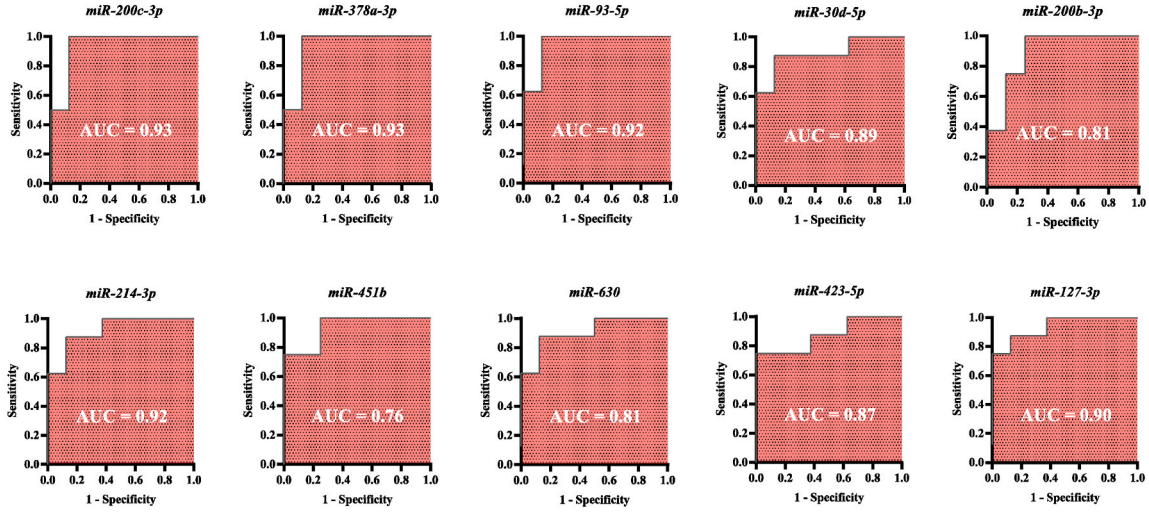

Fig. 8. Visualization of the top 10 differentially expressed miRNAs in epithelial ovarian cancer and receiver operating characteristic (ROC) analysis. **A** Shows validation of miRNA between pre-existing mRNA in EOC vs. OV and predicted miRNAs based on hub genes. **B** Illustrates the 10 top validated miRNAs based on the transcriptomic profile of GSE216150. **C** Illustrates a clustering heatmap of 10 top validated miRNAs. **D** Scatter plots show the gene expression profile of 10 top validated miRNAs in EOC vs. OV. **p-value* < 0.05, ***p-value* < 0.01, and ****p-value* < 0.001. **E** Illustrates ROC curve analysis for selected miRNAs in EOC.

normal tissues of the ovary within the Human Protein Atlas.

IQGAP3 is another hub gene that also appeared as a candidate tumor progression driver. Proteins of the IQGAP family are involved in cytoskeletal functions, cell migration, and cell-cell interaction, and the overexpression of IQGAP3 has been found in colorectal and breast carcinomas and is related to aggressive characteristics and poor prognosis [35,36]. As found in these studies, the overexpression of IQGAP3 and poor survival were found also in the current analysis of EOC. The connection between the expression of IQGAP3 and the alteration of the level of EMT proteins observed in other studies could indicate the involvement of IQGAP3 in the mediation of the connection between cytoskeletal changes and EMT-dependent invasion into the ovarian cancer cell model [37].

Nonetheless, DCN (decorin) and PGR (progesterone receptor) acted as putative tumor suppressor genes within the network. Decorin is a small leucine-rich proteoglycan that regulates growth factor and ECM assembly. DCN repression has been shown to stimulate proliferation, invasion, and migration of various cancers and modulate target therapy sensitivity and resistance [38]. Both mRNA and protein expression of DCN are diminished within EOC and are accompanied by poor survival, thus validating the putative tumor suppressor action of DCN, which regulates the ECM and prevents the acquisition of EMT and metastatic characteristics. PGR has also been historically identified as a positive prognostic marker within ovarian carcinomas, with elevated receptor levels correlating with positive outcomes and sensitivity to endocrine manipulation strategies [39]. As shown within former meta-analysis studies, the expression of PGR is reduced within EOC versus normal tissues and underscores the pivotal role of PGR within the regulation of hormone-dependent differentiation and proliferation within the female reproductive tract [40–42]. The integration of hub genes with miRNA predictions and the GSE216150 miRNA dataset yielded a focused panel of ten candidate miRNAs-miR-200c-3p, miR-378a-3p, miR-93-5p, miR-30d-5p, miR-200b-3p, miR-214-3p, miR-451b, miR-630, miR-423-5p, and miR-127-3p that showed significant dysregulation in EOC vs. normal ovarian tissue.

Several of these miRNAs have been previously implicated in EMT, chemoresistance, and prognosis of EOC and other cancers. Of specific interest is the miR-200 family, of which miR-200b-3p and miR-200c-3p are well-known mediators of EMT through the repression of ZEB1 and ZEB2 and maintenance of E-cadherin expression levels [43]. The fact that miR-200c-3p is also up-regulated within EOC and has high diagnostic accuracy (AUC ~ 0.9), similar to those studies that found it to be elevated and correlated with tumor load within the circulation, further verifies the role of the miR-200 family within EOC as a noninvasive biomarker and a modulator of EMT.

MiR-378a-3p and miR-214-3p also shown to be important targets in the current study. MiR-378a-3p has been shown to play a role in chemo sensitivity to platinum and anti-angiogenic treatments, targeting MAPK1/GRB2 and other genes related to apoptosis and cell cycle regulation [44,45]. MiR-214-3p has also been shown to be related to platinum resistance, apoptosis, and EMT and to be part of regulatory networks that include lncRNAs such as PVT1 and XIST, and implicated in ovarian cancer progression [46]. Both miR-378a-3p and miR-214-3p were found to be significantly differently expressed and relatively good predictors of the difference between EOC and normal tissues in the present dataset [44–46]. Although these two microRNAs have not been shown to regulate EMT directly, they represent attractive candidates for further functional studies.

Our drug-gene interaction analysis translated the hub gene network into pathway-based therapeutic hypotheses. Importantly, the identified drug-gene pairs should be interpreted as hypothesis-generating repurposing candidates rather than EMT-specific or EOC-tailored therapeutic recommendations, as no drug sensitivity or EMT-dependent functional validation was performed in this study. Eight clinically relevant drug-gene pairs were prioritized, including the AURKA inhibitor alisertib, topoisomerase II-targeting agents (etoposide, teniposide, epirubicin) against TOP2A, selective estrogen receptor modulators (tamoxifen, toremifene) targeting ESR1, the GnRH agonist goserelin for GNRHR, and the BCL2 inhibitor venetoclax. Most of these agents are already approved for other malignancies, highlighting a degree of translational readiness [47,48].

The concordant directionality between target biology and drug mechanism for example, inhibiting overexpressed AURKA or BCL2 is consistent with a tumor context that favors cell-cycle progression and survival [48]. Although our analysis is based on in silico interactions rather than direct drug response data in EOC, it provides a rational starting point for prioritizing drug–gene axes that intersect EMT and survival pathways.

Overall, our work supports an EMT-centered view of EOC biology in which extracellular matrix remodeling, developmental signaling (WNT/TGFβ/BMP), and specific hub genes and miRNAs jointly orchestrate tumor progression. A key strength of this study is the use of meta-analysis across multiple cohorts, combined with orthogonal validation at the protein level and integration with independent EMT signatures and drug–gene databases. Rather than proposing isolated single-gene markers, we highlight coherent regulatory modules such as AURKA/IQGAP3 centered proliferative and migratory circuits, DCN/PGR–linked protective axes, and miR-200 regulated EMT that can be experimentally tested and potentially exploited therapeutically.

4.1. Limitations

This study has several limitations. First, all analyses were conducted on publicly available microarray datasets with relatively modest sample sizes, which may limit statistical power and generalizability; microarray cohorts and larger, clinically annotated datasets would provide more robust validation. Second, although we applied meta-analytic strategies and harmonized gene symbols across platforms, residual batch effects and platform-specific biases cannot be completely excluded. Third, EMT engagement was inferred from transcriptomic signatures and correlations with EMTome-derived epithelial and mesenchymal scores rather than from direct functional assays, and our findings should therefore be interpreted as hypothesis-generating. Fourth, the immunohistochemistry validation relied on Human Protein Atlas panels derived from different donors rather than paired normal-tumor samples from the same individuals, so protein-level differences reflect population-level rather than within-patient comparisons. Finally, we did not perform experimental validation of the proposed miRNA-mRNA drug axes; in vitro and in vivo studies will be required to confirm their mechanistic roles and therapeutic exploitability in EOC.

5. Conclusion

Using an EMT-focused, systems biology approach, we integrated mRNA and miRNA expression profiles from multiple GEO cohorts to define a consensus transcriptomic signature in epithelial ovarian cancer. We identified a coherent set of dysregulated genes and miRNAs that converge on EMT, extracellular matrix organization, and developmental WNT and TGFβ/BMP signaling, and distilled these into ten hub genes, ten candidate EMT-related miRNAs, and eight clinically relevant drug–gene pairs. Together, these EMT-regulatory axes suggest candidate diagnostic and prognostic biomarkers, as well as pathway-based therapeutic hypotheses, rather than isolated single markers. Future work should validate these mRNA-miRNA drug modules in independent cohorts and functional models, with the aim of translating EMT-centered signatures into clinically actionable tools for risk stratification and targeted therapy in EOC.

CRediT authorship contribution statement

Roozbeh Heidarzadehpilehrood: Writing – review & editing, Writing – original draft, Visualization, Supervision, Software, Project

administration, Methodology, Investigation, Formal analysis, Data curation. **King-Hwa Ling:** Writing – original draft, Visualization, Methodology, Investigation, Formal analysis, Data curation. **Habibah Abdul Hamid:** Writing – original draft, Visualization, Methodology, Investigation, Formal analysis, Data curation.

Availability of data and materials

This research used publicly datasets https://www.ncbi.nlm.nih.gov/geo/, and http://cistrome.org/TIMER/. All data generated and analyzed during this study are included in the research and its supplementary files.

Funding

The authors declare that no funds, grants, or other support were received in this research.

Declaration of competing interest

The authors declare that they have no known competing financial interests or personal relationships that could have appeared to influence the work reported in this paper.

Acknowledgements

Not applicable.

Appendix A. Supplementary data

Supplementary data to this article can be found online at https://doi.org/10.1016/j.adcanc.2026.100178.

Data availability

All data and materials were presented through this article.

References

[1] D.K. Armstrong, et al., Ovarian cancer, version 2.2020, NCCN clinical practice guidelines in oncology, J. Natl. Compr. Cancer Netw. 19 (2) (Feb. 2021) 191–226, https://doi.org/10.6004/JNCCN.2021.0007.

[2] R.J. Kurman, I.M. Shih, The origin and pathogenesis of epithelial ovarian Cancer- a proposed unifying theory, Am. J. Surg. Pathol. 34 (3) (Mar. 2010) 433, https://doi.org/10.1097/PAS.0B013E3181CF3D79.

[3] R.J. Kurman, I.M. Shih, Molecular pathogenesis and extraovarian origin of epithelial ovarian cancer–shifting the paradigm, Hum. Pathol. 42 (7) (2011) 918–931, https://doi.org/10.1016/J.HUMPATH.2011.03.003.

[4] R.F. Ozols, et al., Focus on epithelial ovarian cancer, Cancer Cell 5 (1) (2004) 19–24, https://doi.org/10.1016/S1535-6108(04)00002-9.

[5] L. Kuroki, S.R. Guntupalli, Treatment of epithelial ovarian cancer, BMJ 371 (Nov) (2020), https://doi.org/10.1136/BMJ.M3773.

[6] M. Mokhtarinejad, M. Pirhoushiaran, R. Heidarzadehpilehrood, S. Hesami, F. Azmoudeh-Ardalan, A.S. Farahani, Upregulated long non-coding RNAs TMPO-AS1, DDX11-AS1, and POLE gene expression predict poor prognosis in head and neck squamous cell carcinoma (HNSCC), Gene Rep 36 (Sep. 2024) 101942, https://doi.org/10.1016/j.genrep.2024.101942.

[7] M. Pirhoushiaran, R. Heidarzadehpilehrood, M. Mokhtarinejad, S. Hesami, N. Rezaei, A.S. Farahani, Upregulated PCAT-1 predicts poor prognosis and reduced immune cell infiltration in head and neck squamous cell carcinoma through the miR-145-5p/FSCN-1 axis, Mol. Biol. Rep. 52 (1) (Jan. 2025) 1–19, https://doi.org/10.1007/S11033-024-10208-1, 2025 52:1.

[8] T. Mehrabi, R. Heidarzadehpilehrood, M. Mobasheri, T. Sobati, M. Heshmati, M. Pirhoushiaran, Dysregulated key long non-coding RNAs TP53TG1, RFPL1S, DLEU1, and HCG4 associated with epithelial-mesenchymal transition (EMT) in castration-resistant prostate cancer, Advances in Cancer Biology - Metastasis 13 (Mar. 2025) 100132, https://doi.org/10.1016/J.ADCANC.2025.100132.

[9] A. Al-Kateb, et al., Silencing of long non-coding RNAs MIR22HG, LNCTAM34A, and TP53TG1 triggers Cell survival/proliferation and inhibits apoptosis in women's breast cancer. Advances in Cancer Biology - Metastasis, Feb. 2025 100133, https://doi.org/10.1016/J.ADCANC.2025.100133.

[10] R. Bao, M. Olivier, J. Xiang, P. Ye, X. Yan, The significance of lymph node dissection in patients with early epithelial ovarian cancer, Ann. Ital. Chir. 95 (4) (Aug. 2024) 628–635, https://doi.org/10.62713/AIC.3353.

[11] T. He, et al., Composite score of PD-1 + CD8 + tumor-infiltrating lymphocytes and CD57 + CD8 + tumor ascites lymphocytes is associated with prognosis and tumor immune microenvironment of patients with advanced high-grade serous ovarian cancer, Chin. J. Cancer Res. 37 (1) (Dec. 2025) 73–89, https://doi.org/10.21147/J.ISSN.1000-9604.2025.01.06.

[12] D. Li, et al., Tracing the evolution of sex hormones and receptor-mediated immune microenvironmental differences in prostate and bladder cancers: from embryonic development to disease, Adv. Sci. (Weinh). 12 (13) (Apr. 2025), https://doi.org/10.1002/ADVS.202407715.

[13] Y. Rattanapan, V. Korkiatsakul, A. Kongruang, T. Siriboonpiputtana, B. Rerkamnuaychoke, T. Chareonsirisuthigul, MicroRNA expression profiling of Epithelial Ovarian cancer identifies new markers of tumor subtype, MicroRNA 9 (4) (Jul. 2020) 289–294, https://doi.org/10.2174/2211536609666200722125737.

[14] M. Bhadra, M. Sachan, S. Nara, Current strategies for early epithelial ovarian cancer detection using miRNA as a potential tool, Front. Mol. Biosci. 11 (Apr. 2024) 1361601, https://doi.org/10.3389/FMOLB.2024.1361601/BIBTEX.

[15] V.H.L. Nguyen, C. Yue, K.Y. Du, M. Salem, J. O'Brien, C. Peng, The role of microRNAs in epithelial ovarian cancer metastasis, Int. J. Mol. Sci. 21 (19) (Sep. 2020) 7093, https://doi.org/10.3390/IJMS21197093, 2020, Vol. 21, Page 7093.

[16] S. Ghafouri-Fard, H. Shoorei, M. Taheri, miRNA profile in ovarian cancer, Exp. Mol. Pathol. 113 (Apr. 2020) 104381, https://doi.org/10.1016/J.YEXMP.2020.104381.

[17] G.G. Muralidhar, M.V. Barbolina, The miR-200 family: versatile players in epithelial ovarian cancer, Int. J. Mol. Sci. 16 (8) (Jul. 2015) 16833–16847, https://doi.org/10.3390/IJMS160816833, 2015, Vol. 16, Pages 16833-16847.

[18] V. Kumar, S. Gupta, A. Chaurasia, M. Sachan, Evaluation of diagnostic potential of epigenetically deregulated MiRNAs in epithelial ovarian cancer, Front. Oncol. 11 (Oct. 2021) 681872, https://doi.org/10.3389/FONC.2021.681872/BIBTEX.

[19] C. Pan, et al., Exosomal microRNAs as tumor markers in epithelial ovarian cancer, Mol. Oncol. 12 (11) (Nov. 2018) 1935–1948, https://doi.org/10.1002/1878-0261.12371.

[20] X. Zhao, D.Y. Tang, X. Zuo, T.D. Zhang, C. Wang, Identification of lncRNA–miRNA–mRNA regulatory network associated with epithelial ovarian cancer cisplatin-resistant, J. Cell. Physiol. 234 (11) (Nov. 2019) 19886–19894, https://doi.org/10.1002/JCP.28587.

[21] I.V. Pronina, et al., Dysregulation of lncRNA–miRNA–mRNA interactome as a marker of metastatic process in ovarian cancer, Biomedicines 10 (4) (Apr. 2022) 824, https://doi.org/10.3390/BIOMEDICINES10040824/S1.

[22] J.E. Evangelista, Z. Xie, G.B. Marino, N. Nguyen, D.J.B. Clarke, A. Ma'Ayan, Enrichr-KG: bridging enrichment analysis across multiple libraries, Nucleic Acids Res. 51 (W1) (Jul. 2023) W168–W179, https://doi.org/10.1093/NAR/GKAD393.

[23] P. Shannon, et al., Cytoscape: a software environment for integrated models of biomolecular interaction networks, Genome Res. 13 (11) (Nov. 2003) 2498, https://doi.org/10.1101/GR.1239303.

[24] A. Colaprico, et al., TCGAbiolinks: an R/Bioconductor package for integrative analysis of TCGA data, Nucleic Acids Res. 44 (8) (May 2016) e71, https://doi.org/10.1093/NAR/GKV1507, e71.

[25] M. Uhlen, et al., A pathology atlas of the human cancer transcriptome, Science 357 (6352) (Aug. 2017), https://doi.org/10.1126/science.aan2507.

[26] V. Poltavets, M. Kochetkova, S.M. Pitson, M.S. Samuel, The role of the extracellular matrix and its molecular and cellular regulators in cancer cell plasticity, Front. Oncol. 8 (Oct. 2018) 378027, https://doi.org/10.3389/FONC.2018.00431/FULL. OCT.

[27] T.V. Abakumova, D.R. Dolgova, I.I. Antoneeva, T.P. Gening, I.R. Myagdieva, Y. S. Slesareva, Expression of Wnt/β-Catenin pathway markers in ascites tumor cells in ovarian cancer, Bull. Exp. Biol. Med. 179 (1) (Jul. 2025) 69–73, https://doi.org/10.1007/S10517-025-06438-3, 2025 179:1.

[28] S. Usman, et al., Vimentin is at the heart of Epithelial Mesenchymal Transition (EMT) mediated metastasis, Cancers 2021 13 (19) (Oct. 2021) 4985, https://doi.org/10.3390/CANCERS13194985, 13, Page 4985, vol.

[29] Q. Li, X. Xiao, J. Feng, R. Yan, J. Xi, Machine learning-assisted analysis of epithelial mesenchymal transition pathway for prognostic stratification and immune infiltration assessment in ovarian cancer, Front. Endocrinol. 14 (Jun. 2023) 1196094, https://doi.org/10.3389/FENDO.2023.1196094/BIBTEX.

[30] H. Cardenas, et al., EZH2 inhibition promotes epithelial-to-mesenchymal transition in ovarian cancer cells, Oncotarget 7 (51) (Aug. 2016) 84453–84467, https://doi.org/10.18632/ONCOTARGET.11497.

[31] X. Yi, et al., EZH2-mediated epigenetic silencing of TIMP2 promotes ovarian cancer migration and invasion, Sci. Rep. 7 (1) (Jun. 2017) 3568, https://doi.org/10.1038/s41598-017-03362-z, 2017 7:1.

[32] T.V. Do, et al., Aurora kinase A mediates epithelial ovarian cancer cell migration and adhesion, Oncogene 33 (5) (Jan. 2013) 539–549, https://doi.org/10.1038/onc.2012.632, 2014 33:5.

[33] M. Guo, et al., Increased AURKA promotes cell proliferation and predicts poor prognosis in bladder cancer, BMC Syst. Biol. 12 (Suppl 7) (Dec. 2018), https://doi.org/10.1186/S12918-018-0634-2.

[34] J.A. Pérez-Fidalgo, V. Gambardella, B. Pineda, O. Burgues, O. Piñero, A. Cervantes, Aurora kinases in ovarian cancer, ESMO Open 5 (5) (Oct. 2020), https://doi.org/10.1136/ESMOOPEN-2020-000718.

[35] S. Dongol, et al., IQGAP3 promotes cancer proliferation and metastasis in high-grade serous ovarian cancer, Oncol. Lett. 20 (2) (Aug. 2020) 1179–1192, https://doi.org/10.3892/OL.2020.11664/HTML.

[36] X. Hua, et al., IQGAP3 overexpression correlates with poor prognosis and radiation therapy resistance in breast cancer, Front. Pharmacol. 11 (Jan. 2021) 584450, https://doi.org/10.3389/FPHAR.2020.584450/BIBTEX.

[37] F. Song, Q. Dai, M.O. Grimm, D. Steinbach, The antithetic roles of IQGAP2 and IQGAP3 in cancers, Cancers 15 (4) (Feb. 2023) 1115, https://doi.org/10.3390/CANCERS15041115, 2023, Vol. 15, Page 1115.
[38] C. Zhang, et al., Oncolytic adenovirus-mediated expression of decorin facilitates CAIX-targeting CAR-T therapy against renal cell carcinoma, Mol. Ther. Oncolytics 24 (Mar. 2021) 14–25, https://doi.org/10.1016/J.OMTO.2021.11.018.
[39] J.J. Peluso, X. Liu, M.M. Saunders, K.P. Claffey, K. Phoenix, Regulation of ovarian cancer cell viability and sensitivity to cisplatin by progesterone receptor membrane Component-1, J. Clin. Endocrinol. Metab. 93 (5) (May 2008) 1592–1599, https://doi.org/10.1210/JC.2007-2771.
[40] P. Lee, D.G. Rosen, C. Zhu, E.G. Silva, J. Liu, Expression of progesterone receptor is a favorable prognostic marker in ovarian cancer, Gynecol. Oncol. 96 (3) (Mar. 2005) 671–677, https://doi.org/10.1016/J.YGYNO.2004.11.010.
[41] H. Luo, S. Li, M. Zhao, B. Sheng, H. Zhu, X. Zhu, Prognostic value of progesterone receptor expression in ovarian cancer: a meta-analysis, Oncotarget 8 (22) (May 2017) 36845, https://doi.org/10.18632/ONCOTARGET.15982.
[42] S.L. Grimm, S.M. Hartig, D.P. Edwards, Progesterone receptor signaling mechanisms, J. Mol. Biol. 428 (19) (Sep. 2016) 3831–3849, https://doi.org/10.1016/J.JMB.2016.06.020.
[43] A. Pendlebury, et al., The circulating microRNA-200 family in whole blood are potential biomarkers for high-grade serous epithelial ovarian cancer, Biomed. Rep 6 (3) (Mar. 2017) 319, https://doi.org/10.3892/BR.2017.847.
[44] J. Wang, et al., Tumor-derived miR-378a-3p-containing extracellular vesicles promote osteolysis by activating the Dyrk1a/Nfatc1/Angptl2 axis for bone metastasis, Cancer Lett. 526 (Feb. 2022) 76–90, https://doi.org/10.1016/J.CANLET.2021.11.017.
[45] Z. hong Xu, T. zhu Yao, W. Liu, miR-378a-3p sensitizes ovarian cancer cells to cisplatin through targeting MAPK1/GRB2, Biomed. Pharmacother. 107 (Nov. 2018) 1410–1417, https://doi.org/10.1016/J.BIOPHA.2018.08.132.
[46] C. Yang, et al., Inhibition of miR-214-3p aids in preventing epithelial ovarian cancer malignancy by increasing the expression of LHX6, Cancers (Basel) 11 (12) (Dec. 2019), https://doi.org/10.3390/CANCERS11121917.
[47] D. Jiang, H. Chen, J. Cao, Y. Chen, J. Huang, Y. Weng, AURKA, as a potential prognostic biomarker, regulates autophagy and immune infiltration in nasopharyngeal carcinoma, Immunobiology 228 (2) (Mar. 2023) 152314, https://doi.org/10.1016/J.IMBIO.2022.152314.
[48] R. Du, C. Huang, K. Liu, X. Li, Z. Dong, Targeting AURKA in Cancer: molecular mechanisms and opportunities for Cancer therapy, Mol. Cancer 20 (1) (Jan. 2021) 15, https://doi.org/10.1186/S12943-020-01305-3, 2021 20:1.